6-19-2014

Membrane Inlet Mass Spectrometry Reveals that Ceriporiopsis Subvermispora Bicupin Oxalate Oxidase is Inhibited by Nitric Oxide

Ellen W. Moomaw
Kennesaw State University, emoomaw@kennesaw.edu

Richard Uberto
Kennesaw State University

Tu Chingkuang
University of Florida

Recommended Citation

Moomaw, E. W., Uberto, R., & Tu, C. (2014). Membrane inlet mass spectrometry reveals that Ceriporiopsis subvermispora bicupin oxalate oxidase is inhibited by nitric oxide. Biochemical and biophysical research communications, 450(1), 750-754.

Biochemical and Biophysical Research Communications 450 (2014) 750–754

Contents lists available at ScienceDirect

Biochemical and Biophysical Research Communications

journal homepage: www.elsevier.com/locate/ybbrc

Membrane inlet mass spectrometry reveals that *Ceriporiopsis subvermispora* bicupin oxalate oxidase is inhibited by nitric oxide

Ellen W. Moomaw [a,*], Richard Uberto [a], Chingkuang Tu [b]

[a] Department of Chemistry and Biochemistry, Kennesaw State University, Kennesaw, GA 30144, USA
[b] Department of Pharmacology and Therapeutics, University of Florida, Gainesville, FL 32610, USA

ARTICLE INFO

Article history:
Received 29 May 2014
Available online 19 June 2014

Keywords:
Oxalate oxidase
Membrane inlet mass spectrometry
Pichia pastoris
Cupin
NO inhibition
Enzyme assay

ABSTRACT

Membrane inlet mass spectrometry (MIMS) uses a semipermeable membrane as an inlet to a mass spectrometer for the measurement of the concentration of small uncharged molecules in solution. We report the use of MIMS to characterize the catalytic properties of oxalate oxidase (E.C. 1.2.3.4) from *Ceriporiopsis subvermispora* (CsOxOx). Oxalate oxidase is a manganese dependent enzyme that catalyzes the oxygen-dependent oxidation of oxalate to carbon dioxide in a reaction that is coupled with the formation of hydrogen peroxide. CsOxOx is the first bicupin enzyme identified that catalyzes this reaction. The MIMS method of measuring OxOx activity involves continuous, real-time direct detection of oxygen consumption and carbon dioxide production from the ion currents of their respective mass peaks. $^{13}C_2$-oxalate was used to allow for accurate detection of $^{13}CO_2$ (m/z 45) despite the presence of adventitious $^{12}CO_2$. Steady-state kinetic constants determined by MIMS are comparable to those obtained by a continuous spectrophotometric assay in which H_2O_2 production is coupled to the horseradish peroxidase catalyzed oxidation of 2,2′-azinobis-(3-ethylbenzthiazoline-6-sulphonic acid). Furthermore, we used MIMS to determine that NO inhibits the activity of the CsOxOx with a K_I of 0.58 ± 0.06 μM.

1. Introduction

The cupin superfamily, defined by a β-barrel fold, is extraordinarily diverse and includes catalytically inactive seed storage proteins, sugar-binding metal-independent epimerases, and metal-dependent enzymes possessing dioxygenase, decarboxylase, and other activities [1–6]. Oxalate oxidase (OxOx, E.C. 1.2.3.4) is a manganese dependent enzyme that catalyzes the oxygen-dependent oxidation of oxalate to carbon dioxide in a reaction that is coupled with the formation of hydrogen peroxide [7–9]. OxOx activity has been detected in a number of crop plants including wheat [4], barley [7,10,11], beet [12,13], and sorghum [14,15]. Plant OxOx enzymes possess a single cupin domain and are, therefore, structurally characterized and classified as monocupins [1–3,5]. The most characterized plant OxOx's are the barley and wheat enzymes which have been recombinantly expressed in *Pichia pastoris* [8,16]. Fungal OxOx activity was reported in *Ceriporiopsis subvermispora*, a white rot basidiomycete fungus able to degrade lignin [17]. Homology modeling indicates that the *C. subvermispora* enzyme (CsOxOx) is the first manganese-containing bicupin enzyme identified that catalyzes oxalate oxidation [18–20]. CsOxOx shares a 49% sequence homology with the bicupin microbial oxalate decarboxylases (OxDC). OxDC catalyzes the carbon–carbon bond cleavage of oxalate to yield carbon dioxide and formate in a reaction in which there is no net oxidation or reduction [18]. Characterizing bicupin oxalate oxidase affords the opportunity to understand how evolutionarily related protein structures modulate disparate chemical reactivities.

The novel chemistry that oxalate degrading enzymes catalyze is poorly understood. This has motivated numerous recent investigations and resulted in a number of mechanistic proposals for the degradation of oxalate by OxOx and OxDC. Common features of these proposals include the binding of oxalate directly to Mn(II), the formation of Mn(III), and a radical intermediate species [8,9,21–23]. A reversible proton-coupled electron transfer that facilitates decarboxylation is proposed to yield a manganese-bound formyl radical. EPR spin-trapping experiments support the existence of an oxalate-derived radical species formed during turnover [19]. In the absence of an active site proton donor, it has been proposed that OxOx proceeds through a percarbonate intermediate

Abbreviations: OxOx, oxalate oxidase; OxDC, oxalate decarboxylase; CsOxOx, OxOx from *Ceriporiopsis subvermispora*; HRP, horseradish peroxidase; ABTS, 2,2′-azinobis-(3-ethylbenzthiazoline-6-sulphonic acid).

* Corresponding author. Fax: +1 (770) 302 4357.
E-mail address: emoomaw@kennesaw.edu (E.W. Moomaw).

http://dx.doi.org/10.1016/j.bbrc.2014.06.040
0006-291X/

before the second mole of carbon dioxide is released. Conversely, in OxDC from *Bacillus subtilis*, an active site glutamic acid is proposed to protonate the manganese-bound formyl radical before formate is released [22].

In membrane inlet mass spectrometry (MIMS), compounds are introduced to the mass spectrometer from solution through a semipermeable membrane. Sensitivity and simplicity are key attributes of the MIMS method that have led to its application to diverse samples such as pharmaceutical products, bioreactors, and environmental samples [24]. This technique has been used in studies of carbonic anhydrase [25] and OxDC [26]. We report here the use of MIMS to characterize the catalytic properties of oxalate oxidase through the direct and continuous detection of oxygen and carbon dioxide; in addition, we have measured inhibition by NO of the catalytic activity of CsOxOx.

2. Materials and methods

2.1. Materials

Unless otherwise stated, all chemicals and reagents were purchased from Fisher Scientific or Sigma–Aldrich and were of the highest available purity. $^{13}C_2$-oxalate was purchased from Cambridge Isotope Laboratories. Protein concentration was determined using a modified Lowry assay (Pierce) using bovine serum albumin as a standard [27].

2.2. Recombinant bicupin oxalate oxidase

The expression and purification of recombinant oxalate oxidase as a secreted protein using a *Pichia* expression system was carried out as previously described [19]. The pPICZαA vector and *P. pastoris* X33 were obtained from Invitrogen. The metal content of CsOxOx samples was quantified at the University of Georgia Center for Applied Isotope Studies Chemical Analysis Laboratory on the basis of inductively-coupled plasma mass spectroscopy (ICP-MS) [28]. To prepare samples and blanks for determination of metal content, divalent cations were removed from the final enzyme storage buffer by passing through a 1.5 × 16 cm column containing Chelex 100 (Bio-Rad) in the Na^+ form. Purified protein samples were exchanged into the resulting buffer by washing 2.5 mg samples three times with 10-fold volumes of the "scrubbed" buffer in Centricon or Centriprep 30 (Amicon) concentrators [29]. The final filtrates recovered were used as blanks, which possessed insignificant metal content. CsOxOx samples contained 0.4 mol Mn/monomer. Despite substoichiometric Mn occupancy, the specific activity of recombinant CsOxOx compares favorably with that purified from the fungus [17]. The concentration of the enzyme is equal to the protein content of the solution in the kinetic constants reported here.

2.3. Coupled steady-state kinetic assay

The level of oxalate oxidase activity was determined using a continuous assay in which H_2O_2 production is coupled to the horseradish peroxidase (HRP) catalyzed oxidation of 2,2′-azinobis-(3-ethylbenzthiazoline-6-sulphonic acid) (ABTS) [11]. Reaction mixtures contained 25 U HRP, 5 mM ABTS, 50 mM potassium oxalate, and CsOxOx dissolved in sodium succinate, pH 4.0 (total volume 1.0 mL). Assays were monitored at 650 nm and an extinction coefficient of 10,000 M^{-1} cm^{-1} for the ABTS radical product was assumed in these experiments. Control samples omitted HRP in order to distinguish between H_2O_2 production and any oxalate-dependent dye oxidation activity by CsOxOx. Measurements were made at specific substrate and enzyme concentrations in duplicate, and data were analyzed to obtain the values of V_{max} and V_{max}/K_m by standard computer-based methods [30].

2.4. Membrane inlet mass spectrometry

The mass spectrometer used in the MIMS experiments has described previously [31–33]. The inlet probe was a tubing of 1.5 mm internal diameter with one end connected to the mass spectrometer and the other end containing a gas permeable membrane (Silastic, Dow Corning). Measurements were made with an Extrel EXM-200 quadrupole mass spectrometer. The probe was submerged in solutions contained in a 2 mL reaction vessel that was maintained at 25 °C as detailed previously [33]. Mass spectra were obtained using 70 eV electron impact ionization with an emission current close to 1 mA and source pressures were approximately 1×10^{-6} torr.

The membrane inlet mass spectrometer was calibrated the through the measurement of solutions of known CO_2 concentration prepared by injecting solutions of K_2CO_3/$KHCO_3$ (pH 10.2) into the reaction vessel containing concentrated acetic acid. The ion current at m/z 44 was recorded and plotted versus CO_2 concentration (Supplementary Fig. 1). Similarly, a standard curve for the instrument was constructed for O_2 by recording the average ion currents at m/z 32 in solutions of different O_2 concentrations prepared by dilution/mixing of O_2, or air saturated reaction buffer at 25 °C (not shown). Finally, a standard curve for the instrument was generated for NO by observing the average ion currents at m/z 30 of known concentrations of NO prepared by the reaction of known amounts of $NaNO_2$ in a solution of 2 M HCl and 2% KI.

In the absence of NO, reactions were initiated by the addition of recombinant CsOxOx so that the final enzyme concentrations were 0.12 μM in solutions containing substrate and buffer. In experiments examining the ability of NO to inhibit CsOxOx activity, a solution of 5 mM MAHMA NONOate [34] dissolved in 0.01 M aq. NaOH was injected into the reaction mixture 1 min prior to initiation of the reaction by the addition of enzyme. When the reversibility of NO-dependent OxDC inhibition was investigated, a preparation of deoxyhemoglobin, which binds NO very tightly, was added into the reaction mixture.

3. Results and discussion

3.1. Direct detection of CsOxOx activity

The ability to directly measure product formation and substrate consumption is an advantage over a coupled assay. We investigated the applicability of membrane inlet mass spectrometry for the direct detection of the CsOxOx catalyzed oxidation of oxalate. Previous experiments have shown that the steady-state kinetic parameters of CsOxOx are very sensitive to the buffer in which the assay is performed. Steady-state experiments using the coupled assay carried out in acetate buffer, pH 4.0 yielded a V_{max} value of 21.2 U/mg that compares very favorably with the value obtained previously for the native enzyme [17]. The K_m for oxalate, determined in acetate buffer, was 14.9 mM, which was, however, significantly higher than the 0.1 mM value reported for the native enzyme. When succinate buffer, pH 4.0 is used the K_m for oxalate is 1.5 mM and when citrate buffer, pH 4.0 is used the K_m is 0.1 mM. The apparent K_m value of 0.1 mM in citrate suggests that succinate might be a competitive inhibitor. The V_{max} in citrate is, however, reduced (V_{max} = 8.1 U/mg) and the addition of succinate increases the activity of the citrate inhibited enzyme [19]. Succinate buffer, pH 4.0 was selected for these studies in an effort to maximize the k_{cat} and minimize the K_m. Under these conditions

we measured the production of CO_2 through the m/z 45 peak ($^{13}CO_2$) and the consumption of O_2 through the m/z peak 32. A typical experiment is shown in Fig. 1. The 2.0 mL reaction contained 10 mM $^{13}C_2$–oxalate and was initiated at 2 min by the addition of enzyme. Since the reaction mixture was air equilibrated, dinitrogen is present in an essentially constant amount. Its slight decrease over the course of the experiment represents its movement into the headspace or across the membrane inlet into the mass spectrometer. The response time of the apparatus can be observed to be about 10 s. In order to convert the measured ion currents into reactant and product concentrations and rates, the membrane inlet mass spectrometer was calibrated for CO_2, O_2, and NO as described in the Section 2. The calibration curve constructed by measuring the ion current (arbitrary scale) at m/z 44 of solutions of known CO_2 is shown in Supplementary Fig. 1.

In addition to coupled assays, oxalate oxidase activity has been directly measured by monitoring oxygen consumption by the use of a Clark oxygen electrode [8,23]. Both MIMS method and the oxygen electrode method are sensitive and can used in physiological experiments or cell suspensions. Both methods require routine calibration. The MIMS method, however, offers distinct advantages as it can simultaneously monitor other gaseous species as well as measure isotopically labeled products, allowing much latitude in monitoring effects of inhibitors and changes in reaction conditions.

3.2. Steady-state kinetic characterization of the CsOxOx catalyzed reaction by MIMS

Doubly ^{13}C labeled oxalate was used in order to distinguish the CO_2 generated by CsOxOx from adventitious CO_2 dissolved in the reaction mixtures. The inset in Fig. 2 shows progress curves monitoring the ion current at m/z 45 (accumulation of $^{13}CO_2$) in solution during the CsOxOx catalyzed reaction at various concentrations of oxalate. Reaction mixtures contained 50 mM sodium succinate, pH 4.0 and were air saturated (256 μM O_2). Oxalate concentrations ranged from 0.1 mM to 10 mM and reactions were initiated at 2 min by the addition of enzyme to a final concentration of 0.12 μM. The rate of the uncatalyzed reaction is negligible and initial velocities were determined from the linear portion of slopes (from about 4% to 12% of the completed reaction). These data and were fit using the Michaelis–Menten equation (Fig. 2).

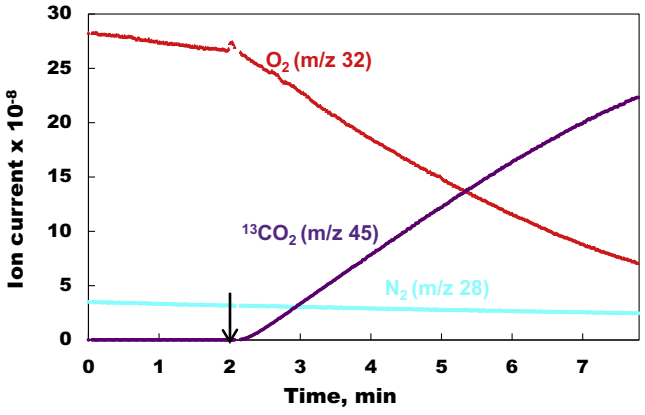

Fig. 1. The production of $^{13}CO_2$ and consumption of O_2 (in arbitrary ion currents) from $^{13}C_2$–oxalate catalyzed by CsOxO. The ion currents for the dissolved gases at their respective peak heights were recorded: purple, $^{13}CO_2$ at m/z 45; red, O_2 at m/z 32; cyan N_2 at m/z 28. The solution contained 50 mM potassium $^{13}C_2$–oxalate and 50 mM sodium succinate buffer at pH 4.0 and 25 °C. The 2 mL reaction was initiated by the addition of recombinant CsOxOx to a final concentration of 0.12 μM at 2 min. (For interpretation of the references to color in this figure legend, the reader is referred to the web version of this article.)

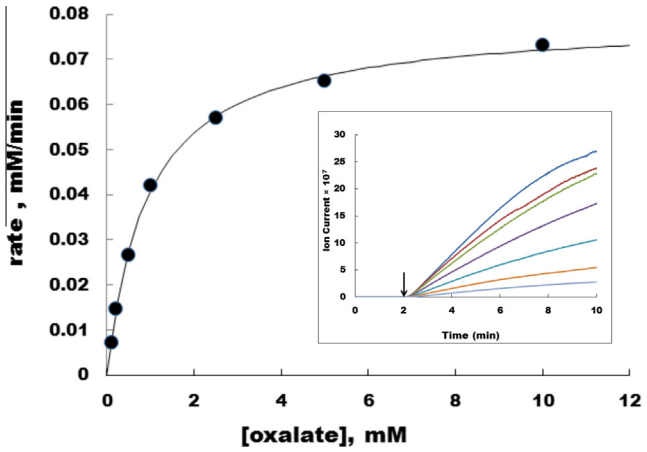

Fig. 2. Oxalate dependence CsOxOx catalyzed oxidation of oxalate. Each data point represents an initial velocity of production of CO_2 measured from the data shown in the inset. The smooth line represents a best fit using the Michaelis–Menten equation with $K_m = 0.93 \pm 0.1$ mM and $V_{max} = 20.3 \pm 0.3$ U mg^{-1} ($k_{cat} = 22.3 \pm 0.3$ s^{-1}). Inset: Progress curves monitoring ion currents at m/z 45 (the accumulation of $^{13}CO_2$) in solution during the CsOxOx catalyzed oxidation of oxalate. Initial concentrations of ^{13}C-labeled oxalate were as follows: light blue, 0.1 mM; orange, 0.2 mM; aqua, 0.5 mM; purple, 1 mM; green, 2.5 mM; red, 5 mM; dark blue, 10 mM. In addition to the varied concentrations of ^{13}C-labeled oxalate, reaction mixtures contained 50 mM sodium succinate, pH 4.0 and were air saturated (256 μM O_2). The reactions were initiated after 2 min by the addition of recombinant CsOxOx to a final concentration of 0.12 μM. (For interpretation of the references to color in this figure legend, the reader is referred to the web version of this article.)

Table 1
Steady-state kinetic parameters for the CsOxOx catalyzed oxidation of oxalate measured by MIMS and the horse radish peroxidase coupled assay.

Assay	K_m (oxalate), mM	k_{cat}, s^{-1}	k_{cat}/K_m, mM^{-1} s^{-1}
MIMS	0.93 ± 0.1[a]	22.3 ± 0.3	24.0 ± 0.4
ABTS	1.5 ± 0.1	20.0 ± 0.4	13.3 ± 0.4

[a] Uncertainties represent standard errors in the fit to the Michaelis–Menten expression.

The kinetic parameters are given in Table 1 along with those determined by the horse radish peroxidase coupled assay. When measured by the MIMS method, the K_m for oxalate is lower and the k_{cat} is slightly higher resulting in higher k_{cat}/K_m which may be the result of increased sensitivity of the MIMS method over the coupled assay.

Progress curves monitoring the accumulation of $^{13}CO_2$ in solution during the CsOxOx catalyzed oxidation of oxalate at varying dioxygen concentrations are shown in Supplementary Fig. 2. Reaction mixtures contained 10 mM ^{13}C-labeled sodium oxalate, 50 mM sodium succinate, pH 4.0 and varying oxygen concentrations and were prepared by diluting/mixing of O_2 and/or air saturated reaction buffer. Initial rates were measured from the linear portion of curves and the dioxygen dependence of the reaction was determined by fitting these data to the Michaelis–Menten equation. The V_{max} value from this fit was 21.0 ± 0.5 U mg^{-1} ($k_{cat} = 23.1 \pm 0.5$ s^{-1}) which is in good agreement with the value obtained from measuring the oxalate dependence of the reaction. The K_m for dioxygen was determined to be less than 70 μM, but could not be determined specifically due in part to the difficulty of manipulating the oxygen concentrations close to the K_m; the majority of the data was collected at oxalate concentrations above the K_m. To our knowledge this is the first report of the K_m for oxygen for CsOxOx. The K_m for oxygen for the barley enzyme was reported to be 460 μM [35].

3.3. Inhibition of the CsOxOx catalyzed oxidation of oxalate by nitric oxide

Given that NO has been shown to be a reversible inhibitor of *B. subtilis* OxDC [36] and the high sequence identity between the two evolutionarily related proteins, we tested the sensitivity of CsOxOx to inhibition by NO. Fig. 3 shows the progress curves measuring the production of $^{13}CO_2$ during the CsOxOx catalyzed reaction at various NO concentrations which were calculated from initial MAHMA NONOate concentrations. The air saturated reaction mixtures contained 10 mM ^{13}C-labeled sodium oxalate, 50 mM sodium succinate, pH 4.0 and were initiated after 1 min by the addition of recombinant CsOxOx. Catalyzed rates were determined at concentrations of NO ranging from 0.5 to 10 μM. The rates of oxalate oxidation in the presence of NO were fit to a simple Langmuir binding isotherm (Fig. 4), resulting in an inhibition constant K_I of 0.58 ± 0.06 μM. The K_I value for CsOxOx represents two orders of magnitude greater affinity for NO than that of *B. subtilis* OxDC [36] which has a K_I value of 40 μM. Oxygen is required but is not consumed in the decarboxylation reaction catalyzed by OxDC that results in no net oxidation or reduction [9]. The K_m for oxygen of OxDC is 28 ± 8 μM as measured by the dependence of decarboxylase on oxygen concentration [22]. In preliminary experiments to test whether or not the inhibitory effect of NO on the oxidation of oxalate is reversible (not shown), relative peak areas for $^{13}CO_2$ (m/z 45), O_2 (m/z 32), and NO (m/z 30) were monitored. Upon addition of the enzyme the $^{13}CO_2$ peak increased as the O_2 peak decreased. When NO was introduced by the addition of MAHMA NONOate, the NO peak increased, O_2 stopped being consumed, and $^{13}CO_2$ was not produced. Carbonic anhydrase free deoxyhemoglobin (stored in nitrogen atmosphere) was then added. Deoxyhemoglobin binds both NO and O_2, effectively removing them from solution. A subsequent rise in the $^{13}CO_2$ peak was observed suggesting that the inhibition of CsOxOx by NO was reversed by the removal of NO from the reaction mixture.

The simplest explanation for the observed NO CsOxOx inhibition is that NO inhibits the enzyme activity by binding directly to one or both of the Mn centers. We are eager to confirm this hypothesis or seek alternative explanations through further experimentation. X-band EPR experiments with OxDC could not provide direct evidence for NO binding directly to the Mn centers and raised the possibility that the enzyme has a dioxygen binding site [36]. In conclusion, we have demonstrated the use of membrane inlet mass spectrometry provides a rapid, sensitive, direct method to study the oxalate oxidase catalyzed oxidation of oxalate and we have used this technique to reveal that the enzyme is inhibited by NO.

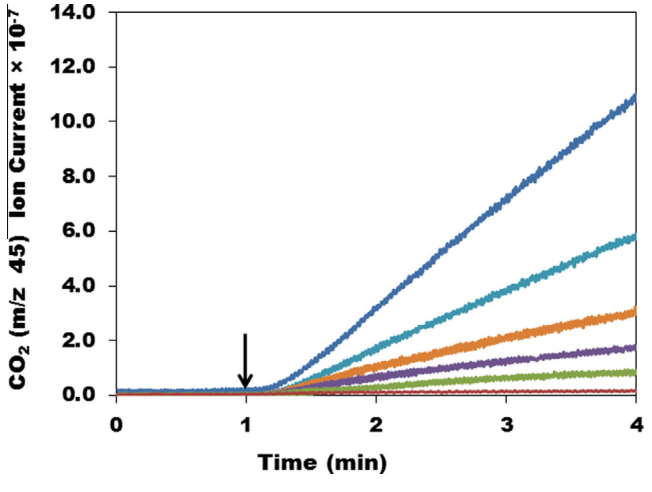

Fig. 3. Progress curves monitoring the accumulation of $^{13}CO_2$ in solution during the CsOxOx catalyzed oxidation of oxalate at varying NO concentrations. Reaction mixtures were air saturated, contained 10 mM ^{13}C-labeled sodium oxalate, 50 mM sodium succinate, pH 4.0, and varying NO concentrations were calculated from initial MAHMA NONOate concentrations. Reactions were initiated after 1 min by the addition of recombinant CsOxOx to a final concentration of 0.12 μM. Initial concentrations of NO were as follows: blue, 0 μM; aqua, 0.5 μM; orange, 1.0 μM; purple, 2.0 μM; green, μM; red, 10 μM. (For interpretation of the references to color in this figure legend, the reader is referred to the web version of this article.)

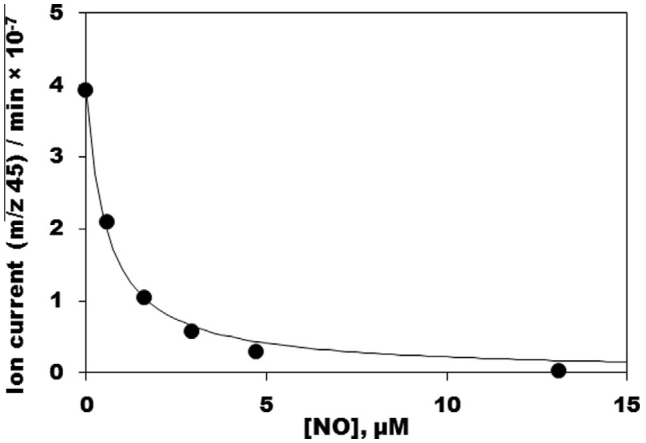

Fig. 4. Inhibition of the CsOxOx catalyzed oxidation of oxalate by nitric oxide. Each data point represents an initial velocity measurement of production of CO_2 from the data of Fig. 3. The rates of oxalate oxidation in the presence of NO were fit to a simple Langmuir binding isotherm, giving an inhibition constant K_I of 0.58 ± 0.06 μM.

Acknowledgments

We thank Dr. David N. Silverman of the University of Florida for allowing us to carry out these experiments in his laboratory and for thoughtful discussions of this research. This work was supported by the National Science Foundation (MCB-1041912) to E.W.M.

Appendix A. Supplementary data

Supplementary data associated with this article can be found, in the online version, at http://dx.doi.org/10.1016/j.bbrc.2014.06.040.

References

[1] J.M. Dunwell, A. Purvis, S. Khuri, Cupins: the most functionally diverse protein superfamily?, Phytochemistry 65 (2004) 7–17
[2] J.M. Dunwell, S. Khuri, P.J. Gane, Microbial relatives of the seed storage proteins of higher plants: conservation of structure and diversification of function during evolution of the cupin superfamily, Microbiol. Mol. Biol. Rev. 64 (2000) 153–179.
[3] J.M. Dunwell, P.J. Gane, Microbial relatives of seed storage proteins: conservation of motifs in a functionally diverse superfamily of enzymes, J. Mol. Evol. 46 (1998) 147–154.
[4] J.M. Dunwell, Cupins: a new superfamily of functionally diverse proteins that include germins and plant storage proteins, Biotechnol. Genet. Eng. Rev. 15 (1998) 1–32.
[5] J.M. Dunwell, A. Culham, C.E. Carter, C.R. Sosa-Aguirre, P.W. Goodenough, Evolution of functional diversity in the cupin superfamily, Trends Biochem. Sci. 26 (2001) 740–746.
[6] R. Uberto, E.W. Moomaw, Protein similarity networks reveal relationships among sequence, structure, and function within the cupin superfamily, PLoS One 8 (2013) e74477.
[7] V.P. Kotsira, Y.D. Clonis, Oxalate oxidase from barley roots: purification to homogeneity and study of some molecular, catalytic, and binding properties, Arch. Biochem. Biophys. 340 (1997) 239–249.
[8] M.M. Whittaker, J.W. Whittaker, Characterization of recombinant barley oxalate oxidase expressed by *Pichia pastoris*, J. Biol. Inorg. Chem. 7 (2002) 136–145.
[9] D. Svedruzic, S. Jonsson, C.G. Toyota, L.A. Reinhardt, S. Ricagno, Y. Lindqvist, N.G.J. Richards, The enzymes of oxalate metabolism: unexpected structures and mechanisms, Arch. Biochem. Biophys. 433 (2005) 176–192.

[10] J. Chiriboga, Purification and properties of oxalic acid oxidase, Arch. Biochem. Biophys. 116 (1966) 516–523.
[11] L. Requena, S. Bornemann, Barley (Hordeum vulgare) oxalate oxidase is a manganese-containing enzyme, Biochem. J. 343 (Pt 1) (1999) 185–190.
[12] P. Varalakshmi, K.E. Richardson, Studies on oxalate oxidase from beet stems upon immobilization on concanavalin A, Biochem. Int. 26 (1992) 153–162.
[13] A.E. Leek, V.S. Butt, Oxidation of oxalate and formate by leaf peroxisomes, Biochem. J. 128 (1972) 87P.
[14] Satyapal, C.S. Pundir, Purification and properties of an oxalate oxidase from leaves of grain sorghum hybrid CSH-5, Biochim. Biophys. Acta 1161 (1993) 1–5.
[15] C.S. Pundir, N.K. Kuchhal, Satyapal, Barley oxalate oxidase immobilized on zirconia-coated alkylamine glass using glutaraldehyde, Indian J. Biochem. Biophys. 30 (1993) 54–57.
[16] H.Y. Pan, M.M. Whittaker, R. Bouveret, A. Berna, F. Bernier, J.W. Whittaker, Characterization of wheat germin (oxalate oxidase) expressed by *Pichia pastoris*, Biochem. Biophys. Res. Commun. 356 (2007) 925–929.
[17] C. Aguilar, U. Urzua, C. Koenig, R. Vicuna, Oxalate oxidase from *Ceriporiopsis subvermispora*: biochemical and cytochemical studies, Arch. Biochem. Biophys. 366 (1999) 275–282.
[18] M.R. Escutia, L. Bowater, A. Edwards, A.R. Bottrill, M.R. Burrell, R. Polanco, R. Vicuna, S. Bornemann, Cloning and sequencing of two *Ceriporiopsis subvermispora* bicupin oxalate oxidase allelic isoforms: implications for the reaction specificity of oxalate oxidases and decarboxylases, Appl. Environ. Microbiol. 71 (2005) 3608–3616.
[19] P. Moussatche, A. Angerhofer, W. Imaram, E. Hoffer, K. Uberto, C. Brooks, C. Bruce, D. Sledge, N.G. Richards, E.W. Moomaw, Characterization of *Ceriporiopsis subvermispora* bicupin oxalate oxidase expressed in *Pichia pastoris*, Arch. Biochem. Biophys. 509 (2011) 100–107.
[20] E.W. Moomaw, E. Hoffer, P. Moussatche, J.C. Salerno, M. Grant, B. Immelman, R. Uberto, A. Ozarowski, A. Angerhofer, Kinetic and spectroscopic studies of bicupin oxalate oxidase and putative active site mutants, PLoS One 8 (2013) e57933.
[21] O. Opaleye, R.S. Rose, M.M. Whittaker, E.J. Woo, J.W. Whittaker, R.W. Pickersgill, Structural and spectroscopic studies shed light on the mechanism of oxalate oxidase, J. Biol. Chem. 281 (2006) 6428–6433.
[22] M.R. Burrell, V.J. Just, L. Bowater, S.A. Fairhurst, L. Requena, D.M. Lawson, S. Bornemann, Oxalate decarboxylase and oxalate oxidase activities can be interchanged with a specificity switch of up to 282,000 by mutating an active site lid, Biochemistry 46 (2007) 12327–12336.
[23] M.M. Whittaker, H.Y. Pan, E.T. Yukl, J.W. Whittaker, Burst kinetics and redox transformations of the active site manganese ion in oxalate oxidase – implications for the catalytic mechanism, J. Biol. Chem. 282 (2007) 7011–7023.
[24] R.C. Johnson, R.G. Cooks, T.M. Allen, M.E. Cisper, P.H. Hemberger, Membrane introduction mass spectrometry: trends and applications, Mass Spectrom. Rev. 19 (2000) 1–37.
[25] J. Delacruz, R. Mikulski, C. Tu, Y. Li, H. Wang, K.T. Shiverick, S.C. Frost, N.A. Horenstein, D.N. Silverman, Detecting extracellular carbonic anhydrase activity using membrane inlet mass spectrometry, Anal. Biochem. 403 (2010) 74–78.
[26] M.E. Moral, C. Tu, N.G. Richards, D.N. Silverman, Membrane inlet for mass spectrometric measurement of catalysis by enzymatic decarboxylases, Anal. Biochem. 418 (2011) 73–77.
[27] O.H. Lowry, N.J. Rosebrough, A.L. Farr, R.J. Randall, Protein measurement with the folin phenol reagent, J. Biol. Chem. 193 (1951) 265–275.
[28] J.A. Olivares, Inductively-coupled plasma mass spectrometry, Methods Enzymol. 158 (1988) 205–232.
[29] J.C. Gonzalez, K. Peariso, J.E. Penner-Hahn, R.G. Matthews, Cobalamin-independent methionine synthase from *Escherichia coli*: a zinc metalloenzyme, Biochemistry 35 (1996) 12228–12234.
[30] W.W. Cleland, Statistical analysis of enzyme kinetic data, Methods Enzymol. 62 (1979) 151–160.
[31] D.N. Silverman, Carbonic anhydrase: oxygen-18 exchange catalyzed by an enzyme with rate-contributing proton-transfer steps, Methods Enzymol. 87 (1982) 732–752.
[32] R. Mikulski, C. Tu, E.R. Swenson, D.N. Silverman, Reactions of nitrite in erythrocyte suspensions measured by membrane inlet mass spectrometry, Free Radic. Biol. Med. 48 (2010) 325–331.
[33] C. Tu, E.R. Swenson, D.N. Silverman, Membrane inlet for mass spectrometric measurement of nitric oxide, Free Radic. Biol. Med. 43 (2007) 1453–1457.
[34] K.M. Davies, D.A. Wink, J.E. Saavedra, L.K. Keefer, Chemistry of the diazeniumdiolates. 2. Kinetics and mechanism of dissociation to nitric oxide in aqueous solution, J. Am. Chem. Soc. 123 (2001) 5473–5481.
[35] M. Kanauchi, J. Milet, C.W. Bamforth, Oxalate and oxalate oxidase in malt, J. Inst. Brewing (2009) 232–237.
[36] M.E. Moral, C. Tu, W. Imaram, A. Angerhofer, D.N. Silverman, N.G. Richards, Nitric oxide reversibly inhibits *Bacillus subtilis* oxalate decarboxylase, Chem. Commun. (Camb.) 47 (2011) 3111–3113.